238 *Inorg. Chem.* **2011**, *50*, 238–244
DOI: 10.1021/ic1018828

Inorganic Chemistry
Article

Synthesis, Structure, and Bonding of $BaTl_4$. Size Effects on Encapsulation of Cations in Electron-Poor Metal Networks.

Jing-Cao Dai,[†,‡] Shalabh Gupta,[†] and John D. Corbett*[,†]

[†] *Ames Laboratory and Department of Chemistry, Iowa State University, Ames, Iowa 50011, United States, and*
[‡] *Institute of Materials Physical Chemistry, Huaqiao University, Xiamen, Fujian 361021, China*

Received September 14, 2010

The synthesis, structure, and bonding of $BaTl_4$ are described [*C2/m*, $Z = 4$, $a = 12.408(3)$, $b = 5.351(1)$, $c = 10.383(2)$ Å, $\beta = 116.00(3)°$]. Pairs of edge-sharing Tl pentagons are condensed to generate a network of pentagonal biprisms along *b* that encapsulate Ba atoms. Alternating levels of prisms along *c* afford six more bifunctional Tl atoms about the waists of the biprisms, giving Ba a coordination number of 16. Each Tl atom is bonded to five to seven other Tl atoms and to three to five Ba atoms. There is also strong evidence that Hg substitutes preferentially in the shared edges of the Tl biprisms in $BaHg_{0.80}Tl_{3.20}$ to generate more strongly bound Hg_2 dimers. Cations that are too small relative to the dimensions of the surrounding polyanionic network make this $BaTl_4$ structure (and for $SrIn_4$ and perhaps $EuIn_4$ as well) one stable alternative to tetragonal $BaAl_4$-type structures in which cations are bound in larger hexagon-faced nets, as for $BaIn_4$ and $SrGa_4$. Characteristic condensation and augmentation of cation-centered prismatic units is common among many relatively cation- and electron-poor, polar derivatives of Zintl phases gain stability. At the other extreme, the large family of Frank−Kasper phases in which the elements exhibit larger numbers of bonded neighbors are sometimes referred to as orbitally rich.

Introduction

Salts between active (group I to III) metals and post-transition (or p-) elements or their polyanions that satisfy longstanding classical octet rules of chemical bonding for the latter are often known at Zintl phases or compounds.[1,2] The left-hand limit in the periodic table for these nominal anions has traditionally been associated with elements in group 14, such that different characteristics appear for the heavier group 13 *triels* Ga, In, Tl[3] and increase to the left. In general, the latter systems possess too few electrons to achieve normal closed-shell valence states in the presence of the same number of valence orbitals. These characteristics are in part related to those for simple metals, which are likewise relatively electron poor (or orbitally rich), and related bonding adjustments occur—increasingly multicentered, delocalized, and less directional, and with higher coordination numbers in extended structures. Interactions among the less electronegative p-elements (or even group 11 or 12 members in Zintl phase derivatives) characteristically generate electron-deficient clusters or networks, virtually every instance exhibiting a novel result in terms of structure and bonding.[3] Indeed, the diverse alkaline-earth-metal−triel compounds may not exist without the additional bonding features achievable with these in extended solids. Additional and particularly important features in what have been termed "polar intermetallics"[4] are the expectedly strong polar interactions between the two component types that afford stronger bonds (greater overlap populations) and long-range Madelung energy terms. Increasing size and packing restraints also apply as the polyanionic components grow in size and complexity and as the relative number of cations vary. In general, the achievement of the largest number of close interactions between the two types of components appears to be especially important in diverse network structures in which the number of encapsulated cations is relatively small. Nonetheless, more detailed calculations also make it clear that some covalence (orbital mixing) between the two opposed components is a reality, particularly with decreased size and increased group number of the individual cations, in opposition to the early assumption that charge transfer in Zintl phases and their approximants was complete.

The degree of involvement or encapsulation of the cations in such phases depends to a substantial degree on their (formal) charge/oxidation state and size of that component

*To whom correspondence should be addressed. E-mail: jcorbett@iastate.edu.

(1) Kauzlarich, S., Ed.; *Chemistry, Structure and Bonding of Zintl Phases and Ions*; VCH Publishers: New York, 1996.
(2) Miller, G. J.; Lee, C.-S.; Choe, W. In *Inorganic Chemistry Highlights*; Meyer, G., Naumann, D., Wesemann, L., Eds.; Wiley-VCH: Weinheim, Germany, 2002; pp 21−53.
(3) Corbett, J. D. *Angew. Chem., Int. Ed.* **2000**, *39*, 670.
(4) (a) Zintl, E.; Goubeau, J.; Dullenkopf, W. *Z. Phys. Chem. A* **1931**, *154*, 1. (b) Corbett, J. D. *Chem. Rev.* **1985**, *85*, 383. (c) Garcia, E.; Corbett, J. D. *Inorg. Chem.* **1988**, *27*, 2907.

 Published on Web 12/07/2010

as well as the overall packing requirements of the structures. Alkali-metal counterions are often, but not always, located more or less outside of the anion aggregate, at least for discrete polyanions, although lithium atoms may bind substitutionally in the triel networks.[5] On the other hand, alkaline-earth-metal atoms (Ae = Ca−Ba) in small to modest proportions are commonly found well encapsulated inside a polyanionic network, often within a pentagonal or hexagonal prismatic polyhedron which has augmented bonding to additional network atoms about their waists to give the cations ~14 to 16 neighbors[6] (~Frank−Kasper polyhedra[7]), as in $(Sr,Ba)Au_2In_2$,[8] $SrAu_4In_4$,[9] or $BaIrIn_4$,[10] for example. Beyond this, the higher fields/stronger bonding achieved with trivalent rare-earth-metal atoms often give rise to more diverse and complex arrays built of less familiar or transferable figures,[11−13] but not always.[14]

The characterization and analysis of the monoclinic $SrIn_4$ structure and its bonding by Seo and Corbett[15] a decade ago drew new attention to some particular problems of packing among the many real or potential members of the high symmetry tetragonal $BaAl_4$ type family (as well as among other related structure types). (The $SrIn_4$ structure type should not be confused with the small monoclinic distortion of the $BaAl_4$-type structure reported for $CaGa_4$.[16]) The numerous $BaAl_4$-type systems have subsequently been well analyzed by Haussermann and co-workers.[17] In the $SrIn_4$ case, the centered Sr appears to be too small to support or hold open the 8 + 8 indium polyhedra of condensed 6-rings around Ba, and so forth, in the $BaAl_4$- type structure, and so the structure collapses to the $SrIn_4$ type with 5-rings. (Refinement of X-ray data for the evidently isostructural $ErIn_4$[18] had been reported earlier, but the structure itself was not described or analyzed.) Since then a great deal has been learned about the overall characteristics of analogous but generally ternary polar intermetallics in neighboring systems and the factors that appear to be important in their packing and bonding.[6] We here report the detailed synthesis, structural refinement, and analysis of just the second example for the nominally isostructural $BaTl_4$, which can also be described in terms of condensation of pairs of Ba-centered (and augmented) pentacapped pentagonal prisms of Tl. Structural data are also reported for the isotypic substitution product $BaHg_{0.80}Tl_{3.20}$. Dimensional changes in the latter strongly suggest that the Hg component substitutes in the $BaTl_4$ structure preferentially so as to give dimeric Hg−Hg units in the shared edges between pentagonal prisms. New substitution reactions that yield more $SrIn_4$-type or ternary $BaAl_4$-type structures instead will appear separately.

Experimental Section

Syntheses. The compounds were prepared from high purity elements by the high temperature solid state synthesis techniques described previously.[5,8−10] The reagents were dendritic Ba (99.9%, Alfa-Aesar), Hg (instrument grade, Fisher), Ag (Fisher 99.7%), and Tl granules (99.999%, Alfa-Aesar), which were handled in a N_2-filled glovebox in which the moisture levels were controlled below 0.1 ppm (vol). The surfaces of Ba and Tl were scraped clean with a scalpel before use. The weighed elements were first welded into 9 mm diameter Nb containers, which were then jacketed in evacuated fused silica containers and subsequently heated in resistance furnaces.

Although $BaTl_4$ was first reported in 1965 among a variety of $Ba(Ga, In, Tl)_4$ products, only the existence of an unknown structure was provided for it.[19] In our investigation, weighed Ba−Tl components in welded Ta containers were first homogenized at 1050 °C for 4 h, quenched, and then annealed at 600 °C for 4 d, after which the system was slowly cooled to room temperature. A series of reactions over the composition range $BaHg_xTl_{4-x}$, $0.2 \leq x \leq 1.0$, was similarly loaded and reacted first at 730 °C for 24 h, quenched, equilibrated at 400 °C for 48 h, and then slowly cooled. The latter group all showed SrIn4/BaTl4-type powder patterns with decreased volumes with increasing x. Some degree of Ag substitution was also established for $BaAg_{0.16}Tl_{3.84}$.

Powder X-ray Diffraction. Powder diffraction investigations were carried out on samples that had been mounted inside the glovebox between two Mylar discs with the aid of a little Apiezon vacuum grease and then clamped in the ring holder. The data were recorded at ~22 °C on a Huber 670 Guinier camera equipped with an area-sensitive detector and Cu Kα radiation (λ = 1.540598 Å) that was regularly calibrated with NBS Si 640b. The step size was set at 0.005°, and the exposure time was 30 min. Least-squares refinements to obtain unit cell parameters were done with the aid of the Rietica program.[20]

Structure Determinations. $BaTl_4$. Powder patterns of the first product with this composition indicated a compound that was possibly isostructural with $SrIn_4$. Several silvery single crystals from a later synthesis were selected under low magnification in a glovebox designed for this purpose and mounted in glass capillaries. Data were collected from one at 293(2) K with the aid of a Bruker Smart APEX CCD diffractometer and Mo−Kα radiation (λ = 0.71073 Å). A total of 1818 frames with an exposure time of 10 s each was collected over the complete reciprocal sphere. Intensities were integrated and averaged with the SAINT subprogram in the SMART software package[21] for the probable $C2/m$ monoclinic cell that was indicated by the 804 independent reflections (R_{int} = 0.0878). Of these, 595 reflections were observed [$I > 2\sigma(I)$]. The space group determination by the XPREP program in the SHELXTL 6.1 software package[22] also indicated $C2/m$ was likely.

Empirical absorption corrections were made with SADABS program[23] (μ = 109.78 mm^{-1}). The structure was refined by full-matrix least-squares on F_o^2 with the aid of SHELXTL 6.1 starting with the fractional coordinates of the atoms in $SrIn_4$, ultimately with anisotropic thermal parameters and a secondary extinction parameter. Convergence was obtained at R1 = 4.95% with plausible displacement parameters and no further

(5) Li, B.; Corbett, J. D. *Inorg. Chem.* **2007**, *46*, 6022.
(6) Corbett, J. D. *Inorg. Chem.* **2010**, *49*, 13.
(7) Wells, A. F. *Structural Inorganic Chemistry*, 5th ed.; Clarendon Press: Oxford, 1984; p 1304.
(8) Dai, J.-C.; Corbett, J. D. *Inorg. Chem.* **2007**, *46*, 4592.
(9) Palasyuk, A.; Dai, J.-C.; Corbett, J. D. *Inorg. Chem.* **2008**, *47*, 3128.
(10) Palasyuk, A.; Corbett, J. D. *Inorg. Chem.* **2008**, *47*, 9344.
(11) Galadzhun, Y. V.; Hoffmann, R.-D.; Poettgen, R.; Adam., M. *J. Solid State Chem.* **1999**, *148*, 425.
(12) Zaremba, V. I.; Hlukhyy, V.; Rodewald, U. Ch; Pöttgen, R. *Z. Anorg. Allg. Chem.* **2005**, *631*, 1371.
(13) Zaremba, V. I.; Rodewald, U. Ch.; Lukachuk, M.; Dubenskiy, V. P.; Heying, B.; Katoh, K.; Niide, Y.; Ochiai, A.; Poettgen, R. *Monatsh. Chem.* **2006**, *137*, 249.
(14) Rodewald, U. Ch.; Zaremba, V. I.; Galadzhun, Y. V.; Hoffmann, R.-D.; Pöttgen, R. *Z. Anorg. Allg. Chem.* **2002**, *628*, 2293.
(15) Seo, D.-K.; Corbett, J. D. *J. Am. Chem. Soc.* **2000**, *122*, 9621.
(16) Bruzzone, G.; Fornasini, M. L.; Merlo, F. *J. Less.-Common Met.* **1989**, *154*, 67.
(17) Häussermann, U.; Amerioun, S.; Eriksson, L.; Lee, C.-S.; Miller, G. J. *J. Am. Chem. Soc.* **2002**, *124*, 4371.
(18) Fornasini, M. L.; Ciafici, S. *Z. Kristallogr.* **1990**, *190*, 295.
(19) Bruzzone, G. *Acta Crystallogr.* **1965**, *18*, 1081.
(20) Hunter, B. A. *LHPM-Rietica Rietveld*, Version 1.71; Australian Nuclear Science and Technology Organization: Menai, N. S. W., Australia, 1997.
(21) *SMART*; Bruker AXS, Inc.: Madison, WI, 1996.
(22) *SHELXTL 6.1*; Bruker AXS, Inc.: Madison, WI, 1996.
(23) Blessing, R. H. *Acta Crystallogr.* **1995**, *A51*, 33.

Table 1. Some Crystal and Refinement Data for $BaTl_4$

empirical formula	$BaTl_4$
formula weight	954.82
space group, Z	$C2/m$ (No. 12), 4
unit cell parameters:	
a, b, c (Å);	12.408(3), 5.351(1), 10.383(2);
β (deg); V (Å^3)	116.00(3); 619.6(2)
density(calc.) (Mg/m^3)	10.236
absorp. coeff. (mm^{-1}); R_{int}	109.78; 0.0878
param./restraints/data	32/0/804
R_1, $wR2^a$ ($I > 2\sigma(I)$)	0.0495, 0.1019
(all data)	0.0640, 0.1050
largest diff. peak (e A^{-3})	4.95, −4.42

Table 2. Atomic Coordinates and Isotropic Displacement Parameters (Å^2) for $BaTl_4$

atom	Wyck	x	y	z	U(eq)^a
Ba	4*i* (*.m.*)	0.1816(2)	0	0.7127(2)	0.016(1)
Tl(1)	4*i*	0.1251(1)	0	0.3212(1)	0.021(1)
Tl(2)	4*i*	0.1515(1)	0	0.0416(1)	0.024(1)
Tl(3)	4*i*	0.4045(1)	0	0.5509(1)	0.018(1)
Tl(4)	4*i*	0.4483(1)	0	0.1151(1)	0.025(1)

[a] U(eq) is defined as one-third of the trace of the orthogonalized U_{ij} tensor.

Table 3. Interatomic Distances (Å) in $BaTl_4$

Tl(1)−Tl(2)	3.060(2)	Tl(3)−Ba ×2	4.091(2)
Tl(1)−Tl(3) ×2	3.080(1)	Tl(4)−Tl(2) ×2	3.094(1)
Tl(1)−Tl(3)	3.234(2)	Tl(4)−Tl(3)	3.132(2)
Tl(1)−Tl(4) ×2	3.526(1)	Tl(4)−Tl(4)	3.169(3)
Tl(1)−Ba	3.666(2)	Tl(4)−Tl(2)	3.418(2)
Tl(1)−Ba ×2	3.711(2)	Tl(4)−Tl(1) ×2	3.526(1)
Tl(1)−Ba	3.811(2)	Tl(4)−Ba ×2	3.934(2)
Tl(2)−Tl(1)	3.060(2)	Tl(4)−Ba	4.035(3)
Tl(2)−Tl(4) ×2	3.094(1)	Tl(4)−Ba	4.133(2)
Tl(2)−Tl(4)	3.418(2)	Ba −Tl(2)	3.594(2)
Tl(2)−Tl(2)	3.468(3)	Ba −Tl(3) ×2	3.637(2)
Tl(2)−Ba	3.594(2)	Ba −Tl(2) ×2	3.650(2)
Tl(2)−Ba ×2	3.650(2)	Ba −Tl(1)	3.666(2)
Tl(3)−Tl(3)	2.988(2)	Ba −Tl(1) ×2	3.711(2)
Tl(3)−Tl(1) ×2	3.080(1)	Ba−Tl(1)	3.811(2)
Tl(3)−Tl(4)	3.132(2)	Ba−Tl(3)	3.815(2)
Tl(3)−Tl(1)	3.234(2)	Ba−Tl(4) ×2	3.934(2)
Tl(3)−Ba ×2	3.637(2)	Ba−Tl(4)	4.035(3)
Tl(3)−Ba	3.814(2)	Ba−Tl(3) ×2	4.091(2)
		Ba−Tl(4)	4.133(2)

absorption corrections seemed necessary. The largest residual peak and hole in the ΔF map were 4.95 and −4.42 e·Å^{-3}, close to Tl atoms. Some crystallographic data are summarized in Table 1, and the atom positions and important nearest neighbor distances are listed in Tables 2 and 3, respectively. The anisotropic displacement parameters as well as more detailed crystallographic and refinement information (cif) are available in the Supporting Information.

$BaHg_xTl_{4-x}$. Crystals from the reaction loaded as $x = 0.80$ were selected and mounted in capillaries, and diffraction data from the best was likewise collected on the APEX instrument. A total of 1315 frames with exposures of 10 s per frame were collected at 293(2) K. Intensities were again integrated for the $C2/m$ cell to give 756 independent reflections ($R_{int} = 0.1435$), with 522 observed at the $2\sigma(I)$ level. Refinement starting with the $BaTl_4$ positional data readily converged, eventually at a residual of 5.59% with anisotropic displacement parameters. Of course, there is no hope of distinguishing Hg from Tl with only customary X-ray diffraction data. However, the Hg was assigned to the Tl3 site in $BaTl_4$ because this position (the shared edge) (a) has the smallest ellipsoids and smallest Tl−Tl neighbor distances here and in the parent and (b) shows the largest distance changes from the $BaTl_4$ result on refinement of this ternary, in accordance with the distinct (and logical) size differentiation between Hg and Tl observed in $BaHg_2Tl_2$ and related compounds.[24] It is to be noted that the equivalent Tl1 positions in these two isotypes also have notably larger U_{33} values, suggesting that the U_{ii} data have some real structural meaning.

Band Calculations. The electronic band structure and densities-of-states for $BaTl_4$ were calculated self-consistently by the tight-binding, linear muffin-tin orbital (TB-LMTO) method[25,26] within the atomic spheres approximation (ASA) with the Stuttgart code.[27] Exchange and correlation were treated in the local density approximation, and scalar relativistic effects were taken into account.[28] In ASA, space is filled with overlapping Wigner−Seitz (WS) spheres at each atomic site. An automated procedure is used to optimize the sphere radii, requiring that the overlapping potential be the best possible approximation to the full potential within the limit of 18% overlap between any atom-centered spheres.[29] The WS radii so determined (Å) were Ba, 2.41; Tl1, Tl2, 1.79; Tl3, 1.75; Tl4, 1.83. No empty spheres were necessary for adequate space filling. The basis set utilized 6s, (6p), 5d for Ba and 6s, 6p, 5d, (5f) for Tl, with the downfolded orbitals[30] listed in parentheses. For bonding analysis, the energy contributions of all electronic states for selected atom pairs were calculated as a function of energy according to the crystal orbital Hamilton population (COHP) method.[31] The (average) energy-weighted sums of these up to E_F give −ICOHP values for the individual pairwise Hamilton overlap populations. The −COHP data are plotted with respect to energy as negative values correspond to bonding interactions.

Results and Discussion

Structure. Although the $C2/m$ structure of $BaTl_4$ represented in Figure 1 appears somewhat complex, it originates from a relatively simple motif. This [010] projection along the 5.35 Å b axis is generated by packing of two identical Tl/Ba layers in which all atoms lie on mirror planes at $y = 0$ or 1/2. The two are related by the C-centering ($a/2 + b/2$) operation, as emphasized by their red and orange shadings. The most obvious building unit in each layer is pairs of Tl pentagons that share Tl3−Tl3 edges and lie above and below like pairs of isolated Ba atoms at $y = \pm 1/2$. The shared pentagons are further interconnected within each layer by Tl2−Tl2 and Tl4−Tl4 bonds. These units are replicated within each layer by means of 2-fold axes along b and inversion centers at the cell origin, cell edges, and cell faces for the chosen cell. Particular inversion operations center the internal Tl3−Tl3 edges as well as the Tl2−Tl2 and Tl4−Tl4 bonds that link these dimers. The latter two are most easily recognized in the horizontal planar zigzag chains ...Tl2−Tl2−Tl4−Tl4... that lie around $z = 1/2$ in each layer and run horizontally along a. (An analogue, ... Tl4−Tl3−Tl3−Tl4..., also lies along c.) All Tl−Tl bonds between 2.99 and 3.53 Å are marked, the distances about each Tl varying somewhat irregularly with the number of bonded neighbors, which varies from five (Tl2, Tl3) to seven (Tl4).

A substantial driving force in the formation of this complex polar arrangement (and many others) appears to

(24) Dai, J.-C.; Gupta, S.; Gourdon, O.; Kim., H.-J.; Corbett, J. D. *J. Am. Chem. Soc.* **2009**, *131*, 8677.
(25) Andersen, O. K.; Jepsen, O. *Phys. Rev. Lett.* **1984**, *53*, 2571.
(26) Andersen, O. K. *Phys. Rev.* **1986**, *B34*, 2439.
(27) Tank, R.; Jepsen, O. Burckhardt, H.; Anderson, O. K. *TB-LMTO 47*; Max-Plank-Institut für Festkörperforschung: Stuttgart, Germany, 1994.
(28) Koelling, D. D.; Harmon, B. N. *J. Phys. C* **1977**, *10*, 3107.
(29) Jepsen, O.; Andersen, O. K. *Z. Phys. B* **1995**, *97*, 645.
(30) Lambrecht, W. R. L.; Andersen, O. K. *Phys. Rev. B* **1986**, *34*, 2439.
(31) Dronskowski, R.; Blöchl, P. *J. Phys. Chem.* **1993**, *97*, 8617.

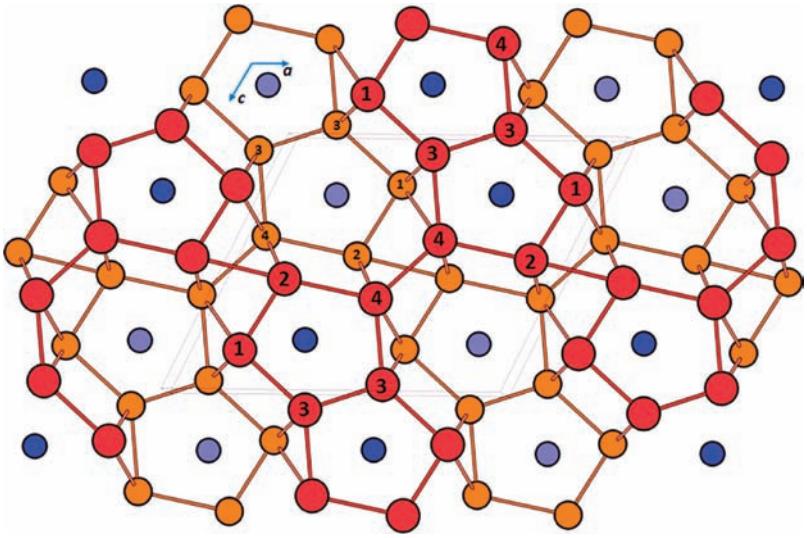

Figure 1. Projection of the monoclinic ($C2/m$) structure of $BaTl_4$ out the 5.351 Å b axis. Red and orange Tl atoms occur in alternating layers at $y = 0, 1/2$. The principal building blocks are pairs of Tl pentagons sharing Tl3−Tl3 edges that are condensed into a 3D array of Ba-centered pentagonal prisms that alternate in depth along a. These are further augmented in the planes of the Ba atoms by Tl atoms in neighboring prisms. This is the smaller cation alternative to the $BaAl_4$-type structure of $BaIn_4$.

be the best accommodation/bonding of the nominal barium cations within/to a complex thallium polyanion that is generally electron-poor (or orbitally rich if the number of valence orbitals is compared with the valence electrons needed to fill them in a classical Zintl sense). The Tl−Tl array is bound principally via its 6 s and 6 p orbitals (below) but not significantly by Tl 5d. Multicenter delocalized bonding is also expected inasmuch as each Tl is bound having by an average of only 3.5 valence electrons after complete charge transfer.[2] The principal feature of the polyanionic construction in Figure 1 is pairs of Ba-centered pentagonal prisms oriented along b and condensed along the view direction via shared basal faces. The prismatic Ba−Tl bonding is also suitably augmented by additional Tl atoms around the prismatic waists that are coplanar with Ba and are members of large 12-rings. The latter are mainly members of basal faces on neighboring pentagonal prisms that have been displaced by $a/2 + b/2$, the C-centering (compare the orange layer in Figure 1). In other words, the condensed pairs of pentagonal prisms that share basal faces along $b = 5.35$ Å are centered by Ba atoms at $b/2$ that also have five or six coplanar Tl neighbors, shared members of basal faces in neighboring pentagonal prisms. The last augmentation is an important part of the total polar Ba−Tl bonding and is common in extended solid state structures, not only in similar situations with encapsulated cations[7−9] but also in the more numerous and familiar examples of condensed tricapped *trigonal* prisms ($PbCl_2$, Fe_2P, etc.).[32] The shared $(Tl3)_4$ faces between pairs of prisms along c are another condensation means to achieve (10 + 5 or 6) Tl neighbors about each Ba even though the overall Tl:Ba proportion is limited to 4:1. The overall structure represents the best solution to a very complex packing/bonding problem. Even larger centering cations could in principle cause a return to the hexagon-based structure of the $BaAl_4$ type, perhaps $RaTl_4$, in parallel with the structure of monoclinic $SrIn_4$ relative to that of tetragonal $BaIn_4$.

A side view of a single $Ba(Tl_5)_2(Tl_6)$ prismatic result is shown in Figure 2 to clarify the geometry about Ba. (Remember that the $(Tl3-Tl3)_2$ prismatic face on the backside is shared with a like partner.) The range of Ba−Tl distances that define the pentagonal prism, 3.64−4.09 Å, is very comparable to the six about the waist, 3.60 to 4.14 Å and with substantially the same average. The last cutoff is somewhat arbitrary; a five-atom limit at 4.04 Å would capture the waist atoms that more or less bridge edges of the pentagonal prisms, whereas the sixth Tl4 at 4.14 Å from Ba is more face capping on the biprism and well bonded only to two other equatorial Tl in this cluster. The position of this last atom is quite sensitive to the relative atom sizes. (A view of the $BaTl_4$ cluster along the pseudo-5-fold axis is shown in the Supporting Information, Figure S3.) All of the surface Tl−Tl bonds span a similar range, 3.06 to 3.42 Å. The equivalent side view of $SrIn_4$ shown in the Supporting Information, Figure S4; it is seen to be more uniformly proportioned and less distorted than $BaTl_4$ Figure 2.

The construction in Figure 1 is completed with the addition of the interlayer bonds, which are otherwise not very noteworthy. Each Tl atom has two additional Tl neighbors in equivalent layers at $\pm b/2$ to yield the basic five-bonded condition (four for Tl1). The inclusion of the longest Tl1−Tl4 interlayer bonds at 3.526(1) Å increases the bonded Tl atoms to six or seven for these two; the few examples of this bond are marked in Figure 1 but not in Figure 2. This longer separation is highly dependent on packing subtleties and disappears from consideration in $BaHg_{0.8}Tl_{3.2}$ and $SrIn_4$ (below).

In general terms, the increase in various measures of relative atomic radii between Sr and Ba is greater than that between In and Tl (because of the lanthanide contraction) whether metallic or ionic radii are considered, for example, differences of 0.07 Å versus 0.02 Å, respectively, in the former type.[33,34] In this sense the cation in

(32) Hyde, B. G.; Andersson, S. *Inorganic Crystal Structures*; J. Wiley & Sons: New York, 1989; p 80.

(33) Pauling, L. *The Nature of the Chemical Bond*, 3rd ed.; Cornell University Press: Ithaca, 1960; p 403.

(34) Shannon, R. D. *Acta Crystallogr.* **1976**, *A32*, 751.

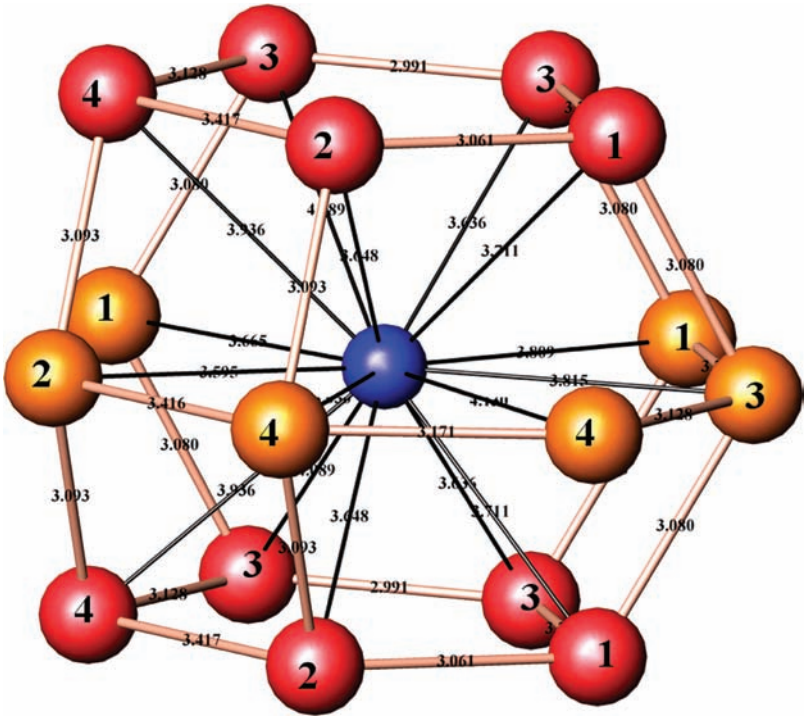

Figure 2. Side view of the $(Tl_5)_2Ba$ pentagonal prism (red) in $BaTl_4$ as augmented by six multifunctional Tl atoms (orange) coplanar with Ba. The longest Tl1−Tl4 bonds (3.526 Å) are omitted.

Table 4. Some Crystal and Refinement Data for $BaHg_{0.80}Tl_{3.20}$

empirical formula	$BaHg_{0.80}Tl_{3.20}$
formula weight	951.83
space group, Z	$C2/m$ (No 12), 4
unit cell param.[a,b]	
a, b, c (Å)	12.229(1), 5.236(1), 10.370(1)
β, V (Å^3)	115.25(1)°, 600.6(2)
density(calc.) (Mg/m^3)	10.523
parameters/restraints/data	32/0/756
R_1, $wR2^a$ ($I > 2\sigma(I)$),	0.0559, 0.1147
(all)	0.0819, 0.1191
largest diff. peak (e A^{-3})	4.942 and −4.187

[a] Powder diffractometer data. [b] Equivalent parameters for $BaHg_{1.00}Tl_{3.00}$: 12.165(1), 5.243(1), 10.380(1) Å; 115.35°; 598.3(2) Å^3, respectively.

$BaTl_4$ should have a relatively tighter fit and the polyanion perhaps be more distorted than in $SrIn_4$, all other factors being disregarded. Indeed, the present cluster unit, Figure 2, is clearly less regular (has a greater range of Ba−Tl distances) than the same cluster in $SrIn_4$ (Supporting Information, Figure S4). For example, the Sr−In distances in the prism, 3.50−3.68 Å, and to the waist atoms, 3.49−3.89 Å, both have narrower ranges, although the d(In−In) range is a little larger, 2.85−3.28 Å.

We have also briefly investigated the early part of the parallel Ba−Hg−Tl system. A particular surprise arose earlier for the unique $BaHg_2Tl_2$ intermetallic in which the two network elements are well differentiated in a tetragonal network of parallel, interbonded chains of condensed Hg hexagons and Tl tetrahedra.[24] The earlier part of this same system $BaHg_xTl_{4-x}$ remains monoclinic up to at least $x = 1.0$, with a 3.4% contraction of the volume of $BaTl_4$ to that point (Table 4) compared with 23.4% for the equivalent $BaHg_2Tl_2$ structure ($x = 2.0$). Although differentiation of the two network elements in the new $BaHg_{0.80}Tl_{3.20}$ structure is impossible by the usual X-ray diffraction means, the refined positional parameters and the distances therein (Tables 4−6) make it quite clear that most if not all of the Hg substitution must occur on the former Tl3 site. This atom type, which defines the shared edges of the pentagonal prisms, already has the smallest displacement ellipsoids and distances to its neighbors in $BaTl_4$. Accordingly, the former Tl3 site now shows both the largest contraction of average distances to its neighbors on substitution of 0.80 Hg/mol, 0.081(2) Å and the smallest average "Tl3−Tl$_n$" distance thereabout, 3.022 Å versus 3.156 Å (and even greater about the other three Tl sites). Thus the unique shared bond between pentagons is now 2.886(3) Å at a presumed ∼80% Hg, 20% Tl occupancy, slightly (0.013(2) Å) less than the average Hg−Hg value in $BaHg_2Tl_2$. These distance differentiations reflect clear distinctions in the bonding of Hg versus Tl, the former exhibiting more important relativistic effects and 5d contributions[24] and, in parallel, a significantly greater Mulliken electronegativity for Hg, 4.91 eV versus 3.2 eV for Tl, and 5.77 for Au.[35] Other irregularities in Ba−Tl distances make further comparison of these in the two structures less certain.

Table 5. Positional ($\times 10^4$) and Isotropic Equivalent Displacement Ellipsoids (Å$^2 \times 10^3$) for $BaHg_{0.80}Tl_{3.20}$

atom	Wyck.	x	y	z	U(eq)
Ba	4i	1748(2)	0	7114(3)	17(1)
Hg[a]	4i	4124(2)	0	5590(2)	21(1)
Tl(1)	4i	1394(2)	0	3362(2)	25(1)
Tl(2)	4i	1496(2)	0	499(2)	32(1)
Tl(3)	4i	4472(2)	0	1150(2)	27(1)

[a] 80% Hg, 20% Tl according to loaded composition. Tl3 position in $BaTl_4$.

(35) Pearson, R. G. *Inorg. Chem.* **1988**, *27*, 736.

Table 6. Interatomic Distances (Å) in $BaHg_{0.80}Tl_{3.20}$

Hg−Hg	2.886(3)	Tl(2)−Ba ×2	3.612(2)
Hg−Tl(1) ×2	3.004(1)	Tl(2)−Ba	3.653(3)
Hg−Tl(3)	3.069(3)	Tl(3)−Hg	3.069(3)
Hg−Tl(1)	3.146(3)	Tl(3)−Tl(2) ×2	3.074(2)
Hg−Ba ×2	3.646(2)	Tl(3)−Tl(3)	3.161(3)
Hg−Ba	3.855(3)	Tl(3)−Tl(2)	3.406(3)
Hg−Ba ×2	3.914(2)	Tl(3)−Tl(1) ×2	3.610(2)
Tl(1)−Hg ×2	3.004(1)	Tl(3)−Ba ×2	3.822(2)
Tl(1)−Tl(2)	3.024(3)	Tl(3)−Ba	4.088(3)
Tl(1)−Tl(3)×2	3.610(2)	Tl(3)−Ba	4.184(3)
Tl(1)−Ba ×2	3.635(2)	Ba−Tl(2) ×2	3.612(2)
Tl(1)−Ba	3.660(3)	Ba−Tl(1) ×2	3.635(2)
Tl(1)−Ba	3.727(3)	Ba−Hg ×2	3.646(2)
Tl(2)−Tl(3) ×2	3.074(2)	Ba −Tl(1)	3.660(3)
Tl(2)−Tl(2)	3.351(4)	Ba−Tl(3) ×2	3.822(2)

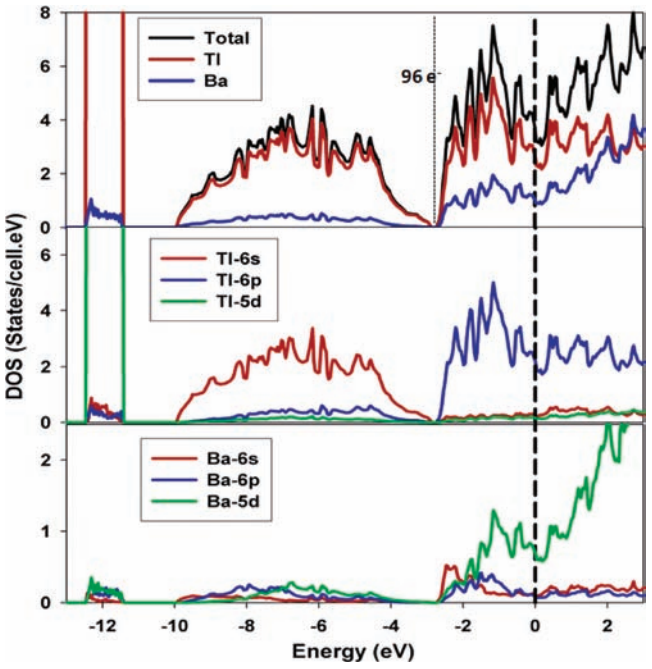

Figure 3. LDA-LMTO-ASA results for $BaTl_4$ as total DOS and as projections of valence orbital PDOS for Tl and Ba. See legends in each section.

Bonding. LMTO calculations for $BaTl_4$ afford some interesting illumination about the bonding in this compound as well as some limited comparisons with that in $BaHg_2Tl_2$.[24] The DOS data and their atomic and orbital projections for $BaTl_4$ are shown in Figure 3, and the −COHP curves (Hamilton populations) for the average pairwise Tl−Tl and Ba−Tl interactions, in Figure 4. Separate 6s and 6p bands in the Tl−Tl bonding are clear (with a calculated 0.11 eV gap), presumably reflecting the greater s−p separation among the sixth period p-elements, and the Tl−Tl bonding is fairly optimized at E_F (IDOS = 1.57 states per atom for Tl 6s; 1.24 for 6p). The Ba−Tl bonding is more skewed toward Tl 6p and with a distinctive Ba 5d contribution to the latter (IDOS = 1.25 total), a fairly common behavior of alkaline-earth elements at this level of theory. Ba−(Hg, Tl) bonding in $BaHg_2Tl_2$ is similar in this limited way (unpublished data).The −ICOHP data for each contact type in $BaTl_4$ are listed in the Supporting Information, and Figure 5 compares these with the respective distance for all Tl−Tl contacts. Relative to other situations, which often involve

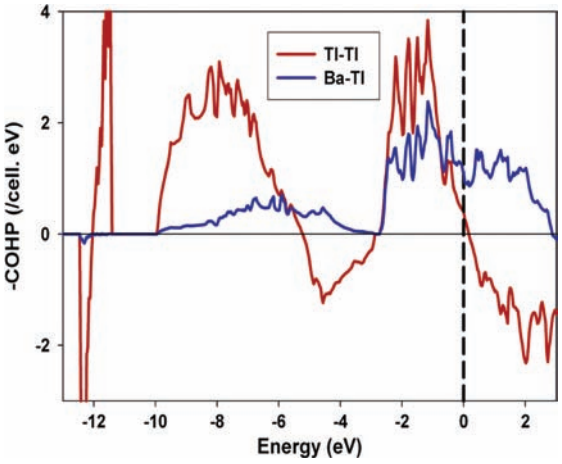

Figure 4. −COHP (Hamilton population) data for Tl−Tl (red) and Ba−Tl (blue) interactions in $BaTl_4$ as a function of energy.

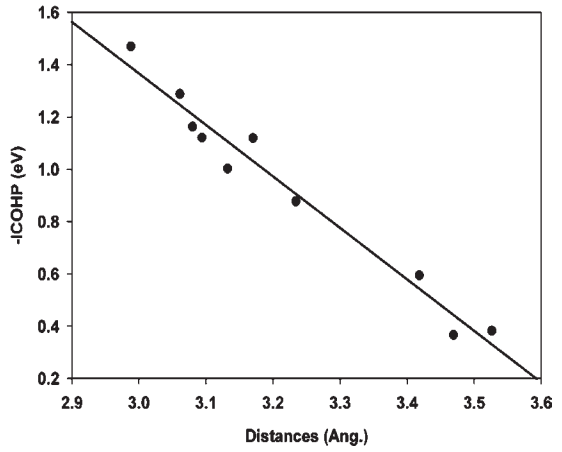

Figure 5. Cumulative −ICOHP data (eV/bond mol) versus the distances of all pairwise Tl−Tl interactions in $BaTl_4$. (Tabulated data in the Supporting Information).

higher-field rare-earth-metals, the scatter or discontinuities in ICOHP values relative to the homoatomic distances are fairly small and few, in contrast to those for Dy_2Te[36] and Y_7Te_2,[37] for example. In other words, there are not any particularly notable geometric or other factors in this polyanion that cause separations to be poorly related to bond populations. The overall structure and bonding in this complex phase can be viewed as fairly ideal or regular despite the evident small distortions.

The bonding in the isotypic $SrIn_4$ was originally examined theoretically only at the extended Hückel level.[15] The later results of subsequent LMTO calculations by Amerioun and Häussermann[38] are qualitatively much more similar to those reported here for $BaTl_4$, but the s−p separation of In states is clearly less than that in $BaTl_4$, as expected.

Tetragonal $BaAl_4$-type structures appear to be the more strongly bound alternative MX_4 structure in this neighborhood when relative atom sizes are suitable, as for

(36) Herle, P. S.; Corbett, J. D. *Inorg. Chem.* **2001**, *40*, 1858.
(37) Castro-Castro, L.; Chen, L.; Corbett, J. D. *J. Solid State Chem.* **2007**, *180*, 3172.
(38) Amerioun, S.; Häussermann, U. *Inorg. Chem.* **2003**, *42*, 7782.

larger cations in the $AeTr_4$ binaries $BaIn_4$,[39] $BaGa_4$, and $SrGa_4$.[19] Simply put, the larger cations in these are more tightly bound between four 6-rings rather than a pair of 5-rings plus augmentation, the former structure giving a larger (8 + 8) number of nominally bonded Tr atoms ("coordination number"). As we see here, the reverse structural change to monoclinic $AeTr_4$ occurs when the larger anion-former Tl is substituted for In in tetragonal $BaIn_4$. (The extreme $SrTl_4$ does not exist, perhaps for packing reasons with the smaller anion.) We have already detailed some relatives of the isotypic monoclinic $SrIn_4$ in which substitution of some smaller atoms in the networks can decrease their sizes, in effect removing the (imagined) unfavorable "rattling" of Sr or in other parallel cases.

The limit of Tl content possible in tetragonal $BaIn_4$ is about $BaIn_{3.37}Tl_{0.63}$,[41] and a new orthorhombic phase intrudes before monoclinic $BaTl_4$ is reached. Substitutions of smaller late 5d transition elements can also be employed to decrease the overall size of the hypothetical tetragonal networks in the unstable $SrIn_4$ and $BaTl_4$ and thereby to stabilize the tetragonal structure even in the presence of other overly large triels. This effect has been known for some time for $BaAuTl_3$[40] and $SrAuIn_3$[8] whereas $BaAuIn_3$[40] $BaPtIn_3$,[41] even $BaHg_{1.3}In_{2.7}$[42] represent even smaller versions of the tetragonal $BaIn_4$ parent.

(39) Wendorff, M.; Röhr, C. *Z. Anorg. Allg. Chem.* **2005**, *631*, 338.
(40) Liu, S.; Corbett, J. D. *Inorg. Chem.* **2004**, *43*, 4988.
(41) Palasyuk, A.; Corbett, J. D. *Z. Anorg. Allg. Chem.* **2007**, *633*, 2563.
(42) Dai, J.-C.; Corbett, J. D., unpublished research.
(43) Li, B.; Corbett, J. D. *Inorg. Chem.* **2007**, *45*, 8812.

Likewise, certain small main-group elements may be substituted into one or the other of two independent Tr lattice sites in the $BaAl_4$-type networks, namely, $(Sr,Ba)(M_x)In_{4-x}$, M = Mg or Zn, $\sim 0.8 \leq x \leq 1.8$, depending on the system.[43] The two Sr−In members are further examples of the stabilization of tetragonal variations of the unknown $SrIn_4$ host. Additional results on related Sr and Ba salts in the Hg−In system and on the new $BaIn_2Tl_2$ will follow. Finally, it is interesting to note that Wendorff and Röhr[39] have identified two binary triel phases in which the presence of only 3-bonded-In in their structures make them rare Zintl phase candidates, SrIn and BaIn.

Acknowledgment. The authors are indebted to Gordon Miller for advice on several theoretical matters. This research was principally supported by the Office of the Basic Energy Sciences, Materials Sciences Division, U.S. Department of Energy (DOE), and was carried out in the facilitates of the Ames Laboratory. The Ames Laboratory is operated for the DOE by Iowa State University under contract No. DE-AC02-07CH11358. J.-C.D. also thanks the NSFC (Grant 50971063) for support.

Supporting Information Available: CIF records and more X-ray parameters and powder pattern data for $BaTl_4$ and $BaHg_{0.80}Tl_{3.2}$; projection of Figure 2 along the pseudo 5-fold axis and a side view of the corresponding $SrIn_4$ figure; tabulated −ICOHP versus distance data for all Tl−Tl pairs in $BaTl_4$. This material is available free of charge via the Internet at http://pubs.acs.org.